AD-A188 236 TRANSIENT SOUND RADIATION FROM INFINITE TWIN PLATE(U) 1/1
ADMIRALTY RESEARCH ESTABLISHMENT TEDDINGTON (ENGLAND)
J H JAMES AUG 87 ARE-TM-(UWA)-87508 DRIC-BR-103398
F/G 20/11 NL

UNCLASSIFIED

END
DATE
FILMED
8

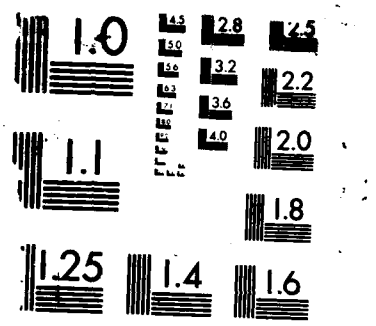

MICROCOPY RESOLUTION TEST CHART

of the excitation; for times t>T+R/c the pressure rises smoothly

TRANSIENT SOUND RADIATION FROM INFINITE THIN PLATE

BY

J H JAMES

Summary

A Fortran program, written by A.G.P. Warham, for calculating the dynamics and acoustics of a thin plate, has been extended to include excitations other than the unit impulse. Numerical results of acoustic radiation demonstrate the usefulness of the program. In the acoustic far-field the transient sound radiation is better computed from a Fourier integral which can be interpreted in terms of drive point and surface radiation, and evaluated numerically by an application of the fast Fourier transform algorithm. Numerical examples are given using both 'thin' and 'thick' plate theories.

32 pages
11 figures

ARE (Teddington)
Queen's Road
TEDDINGTON Middlesex TW11 0LN

August 1987

LIST OF CONTENTS

1. INTRODUCTION

The infinite fluid-loaded plate is one of the prototype problems in the field of fluid-structure interaction, and its time-harmonic response and associated sound radiation have been studied extensively in the acoustic literature. The standard texbook of Junger & Feit [1] gives the mathematics and the physics, and Spicer's [2] intensity vector plots are vivid illustrations of the main features of the acoustic field. The transient dynamics and acoustics of the infinite fluid-loaded plate have not received nearly so much attention despite their importance as canonical problems in underwater acoustics.

Warham [3] has recently written a Fortran computer program for calculating the response of, and sound radiation from, an infinite thin plate which is excited by a unit point impulse. The program cleverly combines analytical and numerical approximations to achieve efficient and accurate computations over a wide range of geometric values and material properties. Many references to previous theoretical work can be found in Warham's comprehensive report.

In the small amount of time set aside for this work it was the aim to (a) extend the range of applicability of Warham's program by giving the user a choice of transient force excitations; (b) give some numerical results of sound radiation which demonstrate that Warham's program is a useful contribution to research in transient fluid-structure interaction; (c) test a stationary phase approximation to the transient pressure in the far-field; and (d) take a first stumble in the direction of developing a software capability for making predictions of transient sound radiation from, and transient sound scattering by, submerged elastic structures.

2. PROBLEM FORMULATION

An infinite plate, see Figure 1, lies in the x,y plane. The upper halfspace contains a fluid and the lower halfspace a vacuum. The plate is excited by a transient stress distribution $F(r,t)$, the plate's normal displacement $W(r,t)$ in bending and the acoustic pressure $p(r,z,t)\equiv p(R,\theta,t)$ being required.

The plate's displacement is assumed to satisfy the thin plate theory of Sophie Germain, viz.

$$D[\partial^2/\partial r^2+(1/r)\partial/\partial r]^2W(r,t)+M\partial^2W(r,t)/\partial t^2 = F(r,t)-p(r,0,t) \qquad (2.1)$$

where $D=Eh^3/12(1-\sigma^2)$ is the plate's flexural rigidity in which E is the Young's modulus, σ is the Poisson's ratio and h is the thickness; $M=\rho_s h$ is the plate's mass per unit area in which ρ_s is the density. The acoustic pressure $p(r,z,t)$ satisfies the wave equation

$$[\partial^2/\partial r^2+(1/r)\partial/\partial r+\partial^2/\partial z^2]p(r,z,t) = \partial^2 p(r,z,t)/c^2\partial t^2 \qquad (2.2)$$

in which c is the velocity of sound in the fluid.

The solution to the above equations proceeds by defining the Fourier-Bessel transform pair for a quantity U(r,z,t), i.e.

$$U(r,z,t) = (1/2\pi)\int_{-\infty}^{+\infty}\int_{0}^{\infty}\bar{U}(\alpha,z,\omega)J_0(\alpha r)\exp(-i\omega t)\alpha d\alpha d\omega$$

$$\bar{U}(\alpha,z,\omega) = \int_{-\infty}^{+\infty}\int_{0}^{\infty}U(r,z,t)J_0(\alpha r)\exp(i\omega t)r dr dt \qquad (2.3)$$

Thus, after defining the plate's displacement W(r,t) and the pressure p(r,z,t) by the transforms

$$W(r,t) = (1/2\pi)\int_{-\infty}^{+\infty}\int_{0}^{\infty}\bar{W}(\alpha,\omega)J_0(\alpha r)\exp(-i\omega t)\alpha d\alpha d\omega \qquad (2.4)$$

$$p(r,z,t) = (1/2\pi)\int_{-\infty}^{+\infty}\int_{0}^{\infty}\bar{p}(\alpha,z,\omega)J_0(\alpha r)\exp(-i\omega t)\alpha d\alpha d\omega \qquad (2.5)$$

it is possible to show that

$$\bar{W}(\alpha,\omega) = \bar{F}(\alpha,\omega)/(D\alpha^4-\omega^2M-i\rho\omega^2/\gamma) \qquad (2.6)$$

$$\bar{p}(\alpha,z,\omega) = -i\rho\omega^2\gamma^{-1}\bar{F}(\alpha,\omega)\exp(i\gamma z)/(D\alpha^4-\omega^2M-i\rho\omega^2/\gamma) \qquad (2.7)$$

in which $\bar{F}(\alpha,\omega)$ is the transform of the transient stress excitation; $\gamma=+(k^2-\alpha^2)^{1/2}$ in order to satisfy the radiation condition; ρ is the fluid's density; and k is the acoustic wavenumber, ω/c. The acoustic momentum relation $\partial p(r,z,t)/\partial z=-\rho\partial^2 W(r,z,t)/\partial t^2$ has been used to ensure continuity of the plate's displacement W(r,t) and the acoustic particle displacement W(r,z,t) at the plate's surface, z=0.

The integrals in equations (2.4-2.5) must be evaluated numerically because closed-form expressions are not available. Mackertich & Hayek [4] have given analytical approximations to the acoustic pressure for the specific case of impulse excitation; however, according to Warham some of their approximations are lacking in accuracy. Despite this (alleged) shortcoming, Makertich and Hayek have identified correctly much of the physics of this transient sound radiation problem.

3. TRANSIENT POINT EXCITATIONS

(a) General

For the particular case of a point force, Q(t), excitation which is located at r=0, viz.

$$F(r,t) = Q(t)\delta(r)/2\pi r \qquad (3.1)$$

the spectral excitation is found from equations (2.3) as

$$\bar{F}(\alpha,\omega) = F(\omega) = (1/2\pi)\int_{-\infty}^{+\infty}Q(t)\exp(i\omega t)dt \qquad (3.2)$$

an excitation which is independent of the wavenumber α.

(b) Impulse

The impulse applied at t=0 is defined as

$$Q(t) = P\delta(t) \tag{3.3}$$

where P is the magnitude of the impulse. Its transform is obtained from equation (3.2) as

$$F(\omega) = P/2\pi \tag{3.4}$$

This is the excitation used in Warham's original Fortran program, which has now been extended to include the transient excitations described in (c)-(g) below.

(c) Sine Wave

The sine wave which is switched on at t=0 and switched off at t=T is defined as

$$Q(t) = F_0\sin(\omega_0 t), \text{ for } 0<t<T \tag{3.5}$$
$$Q(t) = 0, \text{ for } t<0 \text{ and } t>T$$

the time for one cycle being $1/f_0=2\pi/\omega_0$. Its transform is

$$F(\omega) = (F_0/2\pi)[\exp(i\omega T)\{i\omega\sin(\omega_0 T)-\omega_0\cos(\omega_0 T)\}+\omega_0]/(\omega_0^2-\omega^2) \tag{3.6}$$

This excitation taken over a half-cycle is sometimes used to simulate the force due to an elastic impactor.

(d) Squared Sine Wave

The squared sine wave which is switched on at t=0 and off at t=T is defined as

$$Q(t) = F_0\sin^2(\omega_0 t), \text{ for } 0<t<T \tag{3.7}$$
$$Q(t) = 0, \text{ for } t<0 \text{ and } t>T$$

the time for a half-cycle (one loop) being $1/2f_0=\pi/\omega_0$. Its transform is

$$F(\omega) = (F_0/4\pi i\omega)[\exp(i\omega T)-1] \tag{3.8}$$
$$-(F_0/4\pi)[\exp(i\omega T)\{i\omega\cos(\omega_0 T)+2\omega_0\sin(2\omega_0 T)\}-i\omega]/(4\omega_0^2-\omega^2)$$

This excitation, taken over a half-cycle, has been recommended by Akay & Latcha [5] for simulating an elastic impact, because it gives a smoother acceleration response than does the sine wave.

(e) Attenuated Sine Wave

The attenuated sine wave which is switched on at t=0 and off at t=T is defined as

$$Q(t) = F_0 \exp(-at)\sin(\omega_0 t), \text{ for } 0<t<T \qquad (3.9)$$
$$Q(t) = 0, \text{ for } t<0 \text{ and } t>T$$

the time for one cycle being $1/f_0=2\pi/\omega_0$. Its transform is

$$F(\omega) = (F_0/2\pi)[\exp(i\lambda T)\{i\lambda\sin(w_0 T)-\omega_0\cos(\omega_0 T)\}+\omega_0]/(\omega_0^2-\lambda^2) \qquad (3.10)$$

in which $\lambda = \omega+ia$. This is the excitation used by Bolgov & Nikiforov [6] in their analysis of the impact excited infinite plate.

(f) Triangular Pulse

The triangular pulse which is switched on at t=0 and off at t=T is defined as

$$Q(t) = (2F_0/T)t, \text{ for } t=0<t<T/2$$
$$Q(t) = -(2F_0/T)t+2F_0, \text{ for } T/2<t<T \qquad (3.11)$$
$$Q(t) = 0, \text{ for } t<0 \text{ and } t>T$$

Its transform is

$$F(\omega) = (-2F_0/2\pi\omega^2 T)[1-\exp(i\omega T/2)]^2 \qquad (3.12)$$

Nakayama & Nakamura [7] have used this pulse as an acoustic excitation in their work on transient sound radiation from circular plates.

(g) Rectangular Pulse

The square pulse which is switched on at t=0 and off at t=T is defined as

$$Q(t) = F_0, \text{ for } 0<t<T \qquad (3.13)$$
$$Q(t) = 0, \text{ for } t<0 \text{ and } t>T$$

Its transform is

$$F(\omega) = (F_0/2\pi i\omega)[\exp(i\omega T)-1] \qquad (3.14)$$

This pulse can be used to simulate a finite width impulse. It is also the basic component of extended rectangular waveforms, such as the finite length Walsh functions and pseudo random binary sequences. It would not be difficult to add these two waveforms to the list, as their Fourier transforms are known.

4. APPROXIMATION TO FAR-FIELD PRESSURE

(a) Stationary Phase

If the α-integration in equation (2.5) is done by the method of stationary phase [1], then the the far-field pressure

$$p_f(R,\theta,t)=(-\rho/2\pi R)\int_{-\infty}^{+\infty} \omega^2[\bar{F}(\alpha_0,\omega)/G(\alpha_0,\omega)]\exp[-i\omega(t-R/c)]d\omega \tag{4.1}$$

results, where

$$\begin{aligned} G(\alpha_0,\omega) &= D\alpha_0^4-\omega^2M-i\rho\omega^2/\gamma_0 \\ \alpha_0 &= k.\sin(\theta) \\ \gamma_0 &= k.\cos(\theta) \end{aligned} \tag{4.2}$$

The integral, which is invariant with respect to the factor t-R/c, can be evaluated simultaneously for equally spaced time intervals by an application of the fast Fourier transform algorithm. Its use for transient sound radiation calculations does not appear to have been explored in any detail in the acoustics literature.

(b) Physical Interpretation

The integration in equation (4.1) can be done by Cauchy's residue theorem, as there are no branch points to 'muddy the waters'. The function $\bar{F}(\alpha_0,\omega)$ will introduce some complications into the analysis, but it is possible to proceed in a cavalier way by considering only the contribution made by the function $G(\alpha_0,\omega)$, which is responsible for simple poles whose locations are the roots of the reduced cubic equation

$$a_0+a_1\omega+a_3\omega^3= 0 \tag{4.3}$$

where

$$\begin{aligned} a_0 &= -i\rho c/\cos\theta \\ a_1 &= -M \\ a_3 &= (D/c^4)\sin^4\theta \end{aligned} \tag{4.4}$$

At an arbitrary angle θ there are, in the absence of structural damping, three roots of the form

$$\begin{aligned} \omega_1 &= -2i\omega_i \\ \omega_2 &= \omega_r+i\omega_i \\ \omega_3 &= -\omega_r+i\omega_i \end{aligned} \tag{4.5}$$

in which ω_r and ω_i are positive.

For a 5cm thick steel plate with water above and a vacuum

below, with constants as defined in Section 5 below, the values of ω_r and ω_i are

θ	$\omega_r x10^{-3}$	$\omega_i x10^{-3}$	f_r
10	983	2.0	150.1
20	253	2.1	40.3
30	119	2.2	18.9
40	72	2.5	11.4
50	51	3.0	8.1
60	40	3.8	6.4
70	35	5.2	5.5
80	34	8.5	5.4
85	37	12.8	5.9
89	55	26.5	8.7

where $f_r=\omega_r/2\pi$ is the oscillating frequency, in kHz. It is easy to show that the roots may be approximated by the formulae

$$\omega_r = c^2(M/D)^{1/2}/\sin^2\theta$$
$$\omega_i = \rho c/(2M\cos\theta) \qquad (4.6)$$

for values of θ less than 70°, which shows that while ω_r depends on both the mass and stiffness properties of the plate, ω_i is controlled by its mass properties. Enthusiasts of infinite plate problems will recognise the minimum value of ω_r in the approximation, viz. $\omega_c=c^2(M/D)^{1/2}$, as the coincidence frequency, which can be defined as the frequency at which the phase velocity of straight-crested waves, on an unloaded plate, has the value of the speed of sound in the fluid. This frequency is 4.7kHz for a 5cm thick steel plate in water. At frequencies higher than the coincidence frequency there is a strong lobe in the radiated field when time-harmonic conditions prevail, the angle at which the lobe occurs being about $\theta_c=\sin^{-1}(\omega_c/w)^{1/2}$. Thus, it is possible to assign meaning to ω_r as the true frequency of coincidence lobe radiation at the angle θ. See Junger & Feit [1] for a discussion of coincidence lobe radiation.

Three contours of integration are necessary in order to evaluate the Fourier integral analytically:

(1) The first, for $t<0$, is the semicircle in the upper halfplane, the diameter of which runs along the real ω axis, indenting the poles ω_2 and ω_3. Thus, because there are no poles enclosed by this contour the pressure is zero for $t<0$, which is consistent with causality.

(2) The second, for t=0 to R/c, is the semicircle in the upper halfplane, the diameter of which runs along the real ω axis. Thus the poles ω_2 and ω_3 are enclosed by the contour. These poles have no separate existence; rather, they combine to give a real value of pressure which is proportional to $\exp[\omega_i(t-R/c)]\sin[\omega_r(t-R/c)+\phi]$. Bearing in mind that R is infinite in the far-field, this is a pressure whose amplitude increases exponentially with time, from zero to a maximum at t=R/c, and which oscillates at a radian frequency of ω_r.

(3) The third, for t>R/c, is the semicircle in the lower halfplane, the diameter of which runs along the real ω axis. Thus only the pole ω_1 is enclosed, giving an exponentially decreasing pressure proportional to $\exp[-2\omega_i(t-R/c)]$.

When $\theta=0°$ (normal to plate) the coefficient a_3 vanishes, and the only root is

$$\omega_1 = -i(\rho c/M) \qquad (4.7)$$

which lies in the lower halfplane and gives an exponentially decaying pressure field proportional to $\exp[-(\rho c/M)(t-R/c)]$, for t>R/c. Because there are no roots in the upper halfplane the pressure is zero for t<R/c. This root is independent of the plate's stiffness, D, depending only on the fluid's constants and the plate's mass per unit area.

The aforementioned behaviour of the roots can be interpreted physically with the help of the diagram

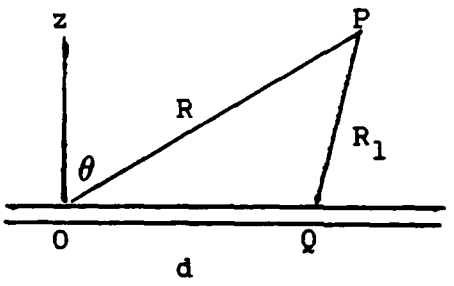

in which it is posible to show that $R_1=R-d.\sin\theta$ in the acoustic far-field. Now consider an energy packet that is injected into the plate at time t=0: some of it will propagate to P via the direct path (OP) in time R/c, and some of it will propagate to P via the indirect path (OQP) in time $d/c_g+R/c-d.\sin\theta/c$, where c_g is the group velocity of the wave packet, in the plate, which is losing energy by radiation. When these two travel times are subtracted it becomes evident that it is possible for energy to arrive at P by the indirect path OQP before it arrives by the direct path OP, provided $c_g>c/\sin\theta$. This is the condition, assuming the group velocity is greater or equal to the phase

velocity, for radiation, at an angle θ, by supersonic straight-crested waves travelling on a fluid-loaded plate. Thus, supersonic waves, on the plate, are the mechanism by which radiation prior to time t=R/c is produced. See Junger & Feit for general details of radiation from wave-bearing surfaces, and Crighton [8] for a full discussion of waves on a fluid-loaded plate.

This non-rigorous treatment of the Fourier integral has shown that the roots of the function $G(\alpha_0,\omega)$ have a physical significance; the first root can be identified with radiation from the excitation point, because it only contributes from time t=R/c, the direct arrival time; the other two roots (in combination) can be identified with surface radiation because they only contribute before time t=R/c, which is only possible if energy has travelled supersonically along the plate surface before radiating into the fluid. Now, as the distance d (see diagram above) along the plate increases, indirect radiation from the plate arrives increasingly earlier than the direct radiation. Furthermore, as d increases, the amplitude of the supersonic wave in the plate will have decreased exponentially because of radiation and structural damping, which means that its radiation will also decrease exponentially, assuming that it is proportional to the the wave's amplitude. As the distance d reduces, it follows that the indirect radiation will increase exponentially until the origin is reached, at which point it merges continuously with the direct radiation.

Precise details of the far-field pressure pulse will depend on the frequency spectrum of the excitation, but general observations are possible for the case of an excitation switched on at time t=0 and then switched off at time t=T. Before the time of the direct arrival, t=R/c, the pressure will oscillate at a frequency whose value is dependent on the angle of observation, the minimum value being close to the coincidence frequency. The amplitude of this pressure will increase exponentially with time until t=R/c, at which time it will merge continuously with the direct pressure. For times t=R/c to t=T+R/c the pressure will be the sum of a relatively smooth direct wave whose travel time is t=R/c, and the oscillating indirect wave which will appear at times to anticipate sharp discontinuities in the excitation. For times t>T+R/c the pressure field will smoothly decay to zero. When $\theta=0°$ the pressure is zero before t=R/c; it is due only to direct radiation at times t=R/c to T+R/c; and it decays smoothly to zero for t>T+R/c. This description of the radiated pulse does not permit the 'ringing', after time t=T+R/c, which was predicted by Mackertich & Hayek; thus it supports Warham's view that their results are in error.

Warham gives explicit formulae for the residue contributions, for the case of impulse excitation, and there is agreement in those areas of the analysis where overlap occurs. It is to be hoped that a proper treatment of the stationary phase approximation and the Fourier integral evaluation by contour integration will be undertaken and reported later.

(c) Timoshenko-Mindlin Plate Theory

An advantage of using the fast Fourier transform algorithm

to evaluate the integral in equation (4.1) is that different plate theories may be used without the complication of finding the roots of the function $G(\alpha_0,\omega)$, which is a simple polynomial only for Sophie Germain plate theory.

For Timoshenko-Mindlin plate theory

$$G(\alpha_0,\omega) = [\{(D\alpha_0^2-\rho_s h^3\omega^2/12)(\alpha_0^2-\rho_s\omega^2/\kappa G)-\rho_s h\omega^2\}/ (1+D\alpha_0^2/\kappa Gh-\rho_s h^2\omega^2/12\kappa G)] - i\rho\omega^2/\gamma_0 \qquad (4.8)$$

in which $G=E/2(1+\sigma)$ and $\kappa=10(1+\sigma)/(12+11\sigma)$. For exact linear plate theory the function $G(\alpha_0,\omega)$ can be found from the work of Spicer [9].

5. NUMERICAL RESULTS

(a) Constants

The numerical results of the transient acoustics of a steel plate in water, shown in Figures 2-11, were obtained using the following material and geometric constants:

Steel Plate:	Young's modulus 19.5×10^{10}
	Poisson's ratio 0.29
	Density 7700.0
	Thickness 0.05
	Hysteretic loss-factor 0.01
Water:	Density 1000.0
(one side only)	Sound velocity 1500.0

The use of a constant hysteretic loss-factor makes the responses non-causal (see Warham for a discussion), but this is barely noticeable in Figures 2-11 . On each plot, where applicable, are marked the times of the direct travel time of the leading edge of the excitation, D=R/c, the minimum indirect acoustic travel time, I=R.cosθ/c, and the direct travel time for the trailing edge of the excitation, L=T+R/c.

(b) Near-field Acoustic Pressure

Figures 2-5 show transient sound radiation versus time, obtained from Warham's program, for various excitations. In each plot the angle of measurement is θ=45°. Because the pressures are in the 'near-field', the physical interpretations of Section 4 will be incomplete since the domains of the subsonic wave and the supersonic 'leaky' wave have been entered - see Crighton [8]. Nonetheless, the results are expected to show certain features that are present in the far-field, viz. an oscillating indirect arrival before t=R/c, and a smooth relaxation to zero after the time of arrival t=T+R/C of the trailing edge of the pulse. In the far-field the indirect arrival oscillates at the frequency ω_r, which has been defined as the true coincidence frequency at the angle of measurement θ, and it has

no well defined beginning. In the near-field the nature of the indirect arrival can be surmised with the help of the diagram of Section 4b, in which the point P is now in the near-field. The first acoustic arrival cannot occur earlier than time $t=R.\cos\theta/c$, via the path OQP in which P is directly above Q; this arrival is associated with an infinite (at least mathematically) value of ω_r. The last indirect acoustic arrival is at time $t=R/c$, via the path OQP in which O and Q are coincident; this arrival is associated with the value of ω_r that corresponds to the angle of observation, e.g. ω_r= 9.5kHz at $\theta=45°$. Thus, the indirect arrival has a well defined beginning, at time $t=R.\cos\theta/c$ where the oscillation frequency is infinite, and ends at time $t=R/c$ with an oscillation frequency of ω_r.

In Figure 2a the excitation is a unit impulse whose frequency spectrum is a constant. The distance R is 1.0m. From the time of the indirect arrival, the pressure increases rapidly with increasing period of oscillation; the oscillations are too rapid to show on the figure. The pressure then decreases with increasing period of oscillation until the time of direct travel when it almost vanishes. These results were obtained with an upper limit of frequency integration set to 1MHz, Warham's program providing an additional contribution by means of an analytical formula. Figure 2b shows the results obtained without the extra analytical contribution. The non-causal behaviour is marked, and the early time arrival parts of the plots differ considerably. When the upper limit of integration is truncated at 10kHz, the maximum level (not shown) is less than unity, which implies the dominance of high frequency surface radiation.

As a test to see whether or not steady-state conditions are reached quickly, a 1kHz and a 10kHz sine wave excitation were switched on for 5 cycles each. The results are shown in Figures 3a and 3b, in which the distance R is 1.0m. The plots show that after an initial transient, time-harmonic conditions prevail within 1 cycle. Spicer [10] has written a Fortran program for calculating near-field pressures due to time-harmonic excitation. This program was used to confirm that the steady-state levels shown in Figures 3a and 3b are exactly as expected.

In order to illustrate the change in pressure shape as a disturbance propagates from the near-field to the far-field, a square wave was switched on for 1/2 millisecond. Figure 4a shows the pressure at R=0.2m. After a small rapidly changing initial transient, at the time of the indirect arrival, the pressure rises rapidly to reach a maximum close to the time of the direct arrival. The pressure then drops smoothly until the indirect arrival part of the 'switch-off' occurs which causes another rapidly varying transient, ending when the pressure drops sharply to a negative value after which it rises smoothly to zero. It is believed that the prevalent feature in the pressure is due to acoustic radiation from the excitation point, and the rapidly varying oscillations are due to radiation from the plate surface. This view is reinforced by the plots shown in Figures 4b, 5a and 5b, which are for R=1, 5 and 25m respectively. The shape of the pressure from the drive point is (possibly) unaltered, but it is masked by oscillations, due to the indirect plate radiation,

which decrease in frequency to about 10kHz, as the distance increases to 25m. According to the Table in Section 4b, the oscillations will have decreased to 9.5kHz by the time the acoustic far-field has been reached. Figure 4b is a vivid illustration of the pressure apparently anticipating the switching on and off of the excitation, which feature is due, of course, to indirect plate radiation.

(c) Far-Field Sound Radiation

A Fortran program has been written to calculate the far-field radiation by evaluating the Fourier integral in equation (4.1) using an application of the fast Fourier transform algorithm. Details of the integration scheme chosen are not given herein. Both Sophie Germain 'thin' and Timoshenko-Mindlin 'thick' plate theories have been included as options in the computer program. Numerical results are shown in Figure 6-11. The levels have been adjusted to the reference distance of 1m, and although the time scale is arbitrary it is useful to know that the the direct arrival time has been set to time t=1ms, by the program, by use of a variable RP whose value is in the graph caption.

Figure 6 shows transient pressures in the far-field when the excitation is a unit impulse. In Figure 6a the angle of observation is $\theta=0°$; the pressure is zero for time $t<R/c$, it is basically a sharp spike at time $t=R/c$, and then it vanishes almost immediately. In Figure 6b the angle of observation is $\theta=45°$; the pressure rises exponentially, with a 9.5kHz modulation, until $t=R/c$, at which time it relaxes smoothly to zero. These plots are in agreement with the physics described and the values tabulated in Section 4b.

As a test to see whether or not steady-state conditions are reached as quickly in the far-field as they are in the near-field, 1kHz and 10kHz sine waves were switched on for 5 cycles each. Figure 7a shows that after an initial transient, oscillating at the frequency of 9.5kHz, as expected, time-harmonic conditions are obtained within 1 cycle for the 1kHz excitation. In Figure 7b the indirect arrival is large because the excitation frequency is close to the frequency of its oscillation. Steady state conditions are in fact reached within 1 cycle, but this is masked by the indirect arrival of the transient generated by the switch-off. Calculations using standard formulae, found in Junger & Feit, have confirmed that the correct steady-state levels have in fact been achieved.

In Figures 8-9 the excitation is a rectangular pulse that has been switched on for 1/2 millisecond. Figure 8a shows the pressure at normal incidence, $\theta=0°$: the pressure, which is zero before time $t=R/c$, rises rapidly as the leading edge reaches the measuring position, drops slowly until the time $t=T+R/c$ of the switch off when it drops rapidly to a negative value, after which it rises smoothly to zero. In Figure 8b the angle of measurement is $\theta=20°$: before $t=R/c$ the indirect arrival due to the leading edge of the excitation is responsible for the exponentially increasing pressure, modulated by an oscillation of about 40kHz; between times $t=R/c$ and $T+R/c$ the direct arrival is modulated by the oscillations of the indirect arrival due to the trailing edge

of the excitation; for times t>T+R/c the pressure rises smoothly to zero. Figures 9a and 9b, for θ=45° and θ=70°, respectively, show similar features, except that the oscillation rates are about 9.5 and 5.5kHz. The physics is well explained by the text and the Table in Section 4. A comparison of Figures 5b (Warham at 25m) and 9a (James in the far-field) shows that these plots are very similar in shape, and in level if Warham's results are referred to 1m using a spherical spreading correction, which reinforces confidence in the correctness of the Fortran programs.

Figure 10 and 11 are comparisons of the transient pressure pulses obtained from the 'thin' and 'thick' plate theories at θ=45°. In Figure 10 the excitation is a rectangular pulse that has been switched on for 1/2 millisecond, the pressure level obtained by using 'thick' plate theory being shown in Figure 10a and the pressure level obtained by using 'thin' plate theory being shown in Figure 10b. The two plots are qualitatively similar; but the 'thick' plate pressure oscillates at a higher frequency than the 'thin' plate pressure, and it has two sharp spikes at its leading and trailing edges. The reason for the former feature is that the frequency ω_r associated with a given aspect θ is higher for 'thick' plate than it is for 'thin' plate theory. The reason for the latter is not understood, but jump discontinuities in the excitation appear to produce more of an overshoot in the acoustic pulse when 'thick' plate theory is used. Also, the Fourier integral is only conditionally convergent, at times t=R/c and t=T+R/c, when 'thick' plate theory is used and the excitation spectrum drops only as fast as $1/\omega$; which means that it is not conclusive that the correct answers are obtained at these times. In Figure 11 the excitation is the triangular pulse on for 1/2 millisecond: the plots are very similar, sharp spikes being absent when 'thick' plate theory is used because there are no jump discontinuities in the excitation.

6. CONCLUDING REMARKS

The limited number of numerical results shown have demonstrated that Warham's program is a valuable contribution to research in transient sound radiation. The program is particularly flexible because it copes with the acoustics (and the dynamics) both at short and long ranges. Its major drawback is its size of almost 9000 lines, and its reliance on library (NAG) subroutines that may not be readily available. In addition to providing bench-mark computations, this Fortran program could be used to investigate:

(a) The build-up and eventual decay of an acoustic energy vortex as a sine wave excitation is switched on, for a time sufficient for time-harmonic response to prevail, and then switched off. Spicer's [2] plots show energy vortices and Waterhouse et al [11] give a condition for their occurrence.

(b) The linear dynamics and acoustics due to impact by an elastic sphere. For this problem, the papers of Akay & Latcha [5], Bolgov & Nikiforov [6] and Heitkämper [12] are relevant.

In the acoustic far-field it is much better to obtain the transient pressure by evaluating numerically a Fourier integral, obtained via a stationary phase approximation, by an application of the fast Fourier transform algorithm. The Fortran program which computes the far-field transient radiation is small, and does not include any proprietary software. Both Sophie Germain and Timoshenko-Mindlin plate theories are included in the program as options, and 'exact' linear theory, of layered media, using the methods of Spicer [9], could be added without too much difficulty. Thus, a comparison of predictions from 'thin', 'thick' and 'exact' theories could be done for transient sound radiation, in much the same way that Clement [13] has done so for the time-harmonic case.

An ad hoc treatment of the contour of integration used to solve the Fourier integral has shown that the poles in the integrand have a physical meaning, viz. direct radiation from the excitation point, arriving at the measuring position at time t=R/c, and indirect radiation from supersonic waves, coming off the surface of the plate at oblique angles, arriving before t=R/c. These features merit rigorous investigation. The numerical results shown are in accordance with the physical interpretation.

7. ACKNOWLEDGEMENT

Thanks are due to A.G.P. Warham, of the National Physical Laboratory, for making available his Fortran computer program and a copy of his report to the Admiralty Research Establishment. The not inconsiderable effort put into the research by Dr Warham is much appreciated.

J.H. James (PSO)
August 1987.

REFERENCES

1. Junger M.C., Feit D., Sound, Structures, and Their Interaction, Second Edition, MIT Press, 1986.

2. Spicer W.J., Acoustic intensity vectors from an infinite plate with line attachments, Admiralty Marine Technology Establishment, Teddington, AMTE(N)TM81086, 1981.

3. Warham A.G.P., Calculation of the effect of a point impact on an infinite elastic plate adjacent to a semi-infinite fluid, National Physical Laboratory, Teddington, Report DITC 80/86, 1986.

4. Mackertich S.S., Hayek S.I., Acoustic radiation from an impulsively excited elastic plate, J.Acoust.Soc.Am., 69(4), 1981, pages 1021-1028.

5. Akay A., Latcha M., Sound radiation from an impact excited clamped circular plate in an infinite baffle, J.Acoust.Soc.Am., 74(2), 1983, pages 640-648.

6. Bolgov V.M., Nikiforov A.S., Transverse impact excited flexural vibrations of an infinite plate, Sov.Phys.Acoust., 26(3), 1980, pages 184-187.

7. Nakayama I., Nakamura A., Transient far-field waveform on the axis of an elastic circular plate excited by a pulsed axial point source, J.Sound Vib., 106(2), 1986, pages 267-274.

8. Crighton D.G., The free and forced waves on a fluid-loaded elastic plate, J.Sound Vib., 63(2), 1979, pages 225-235.

9. Spicer W.J., Free-wave propagation in and sound radiation by layered media with flow, Admiralty Marine Technology Establishment, Teddington, AMTE(N)TM82102, 1982.

10. Spicer W.J., The near-field acoustic pressure of an infinite plate driven by a point force, Admiralty Marine Technology Establishment, Teddington, Unpublished Work, October 1980.

11. Waterhouse R.V., Crighton D.G., Ffowcs-Williams J.E., A criterion for an energy vortex in a sound field, J.Acoust.Soc. Am., 81(5), pages 1323-1326.

12. Heitkämper, von W., Numerical approximation of sound radiation of impact excited plates, Acoustica, 58(3), 1985, pages 141-148.

13. Clement E.J., Numerical results of acoustic radiation, transmission and reflection of steel plate in water, Admiralty Marine Technology Establishment, Teddington, AMTE(N)TM84037, 1984.

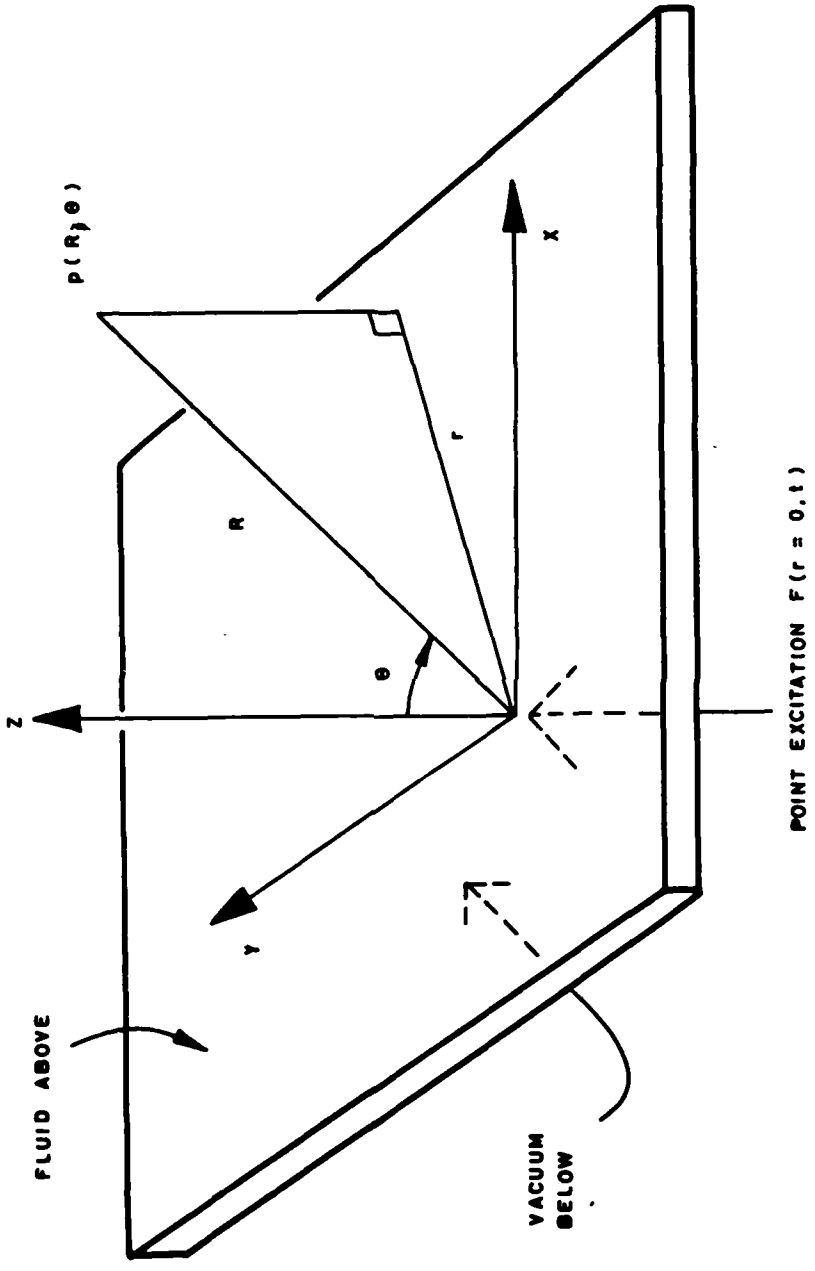

FIG. 1 SECTION OF INFINITE PLATE

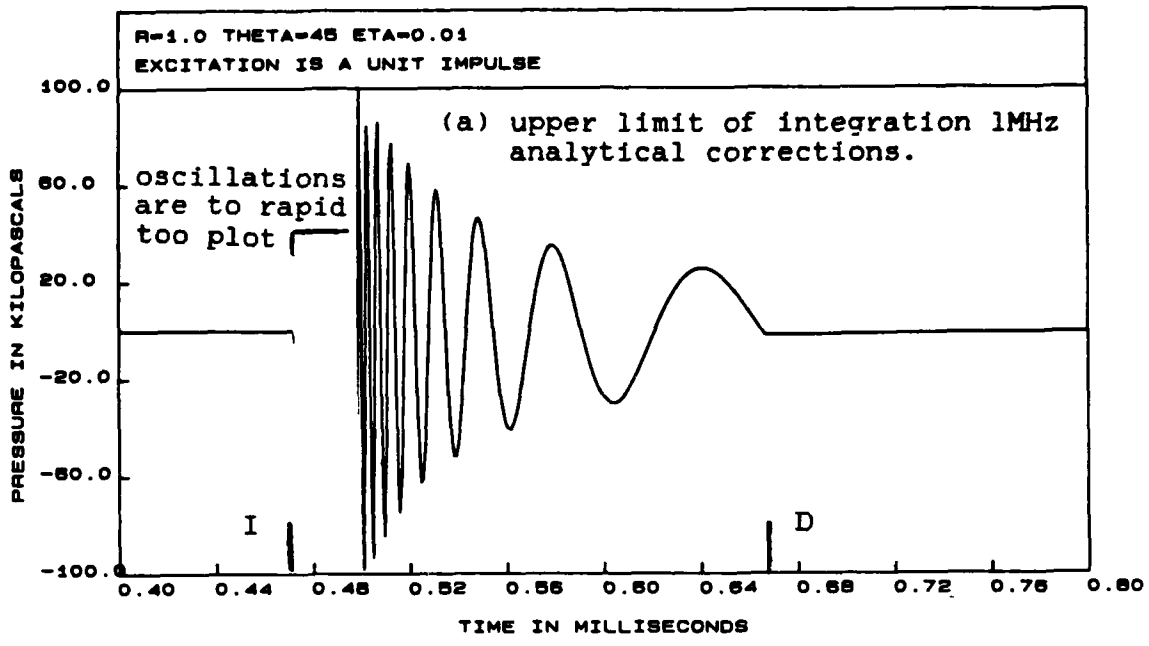

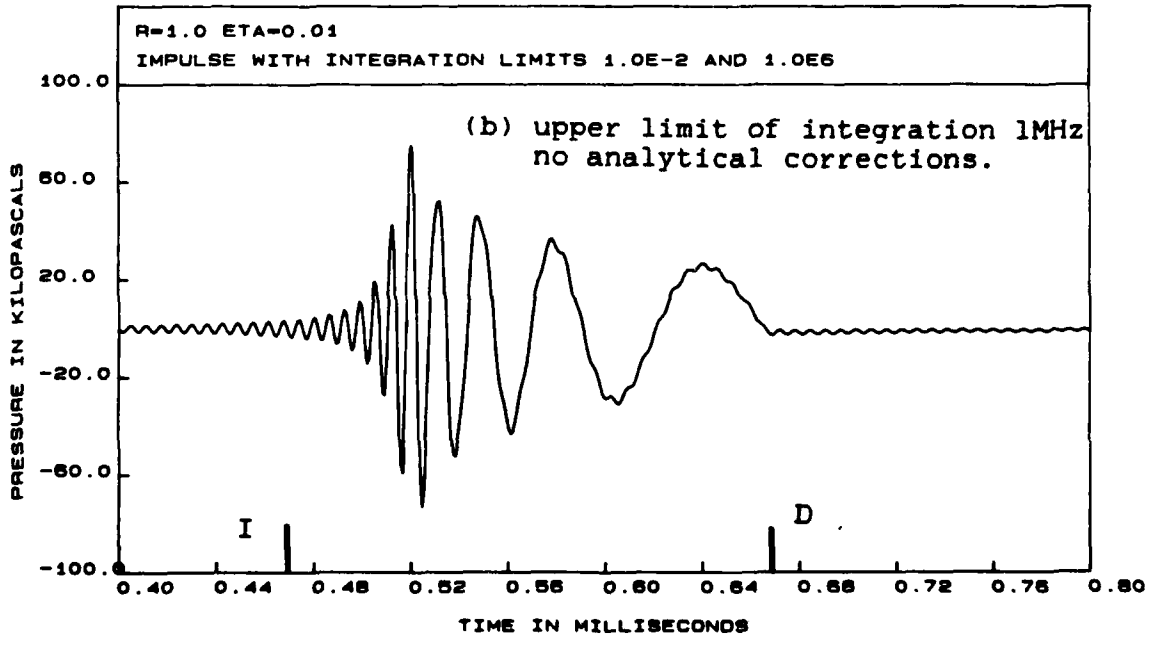

FIG. 2 WARHAM. EXCITATION IS A UNIT IMPULSE
R=1.0m θ=45°

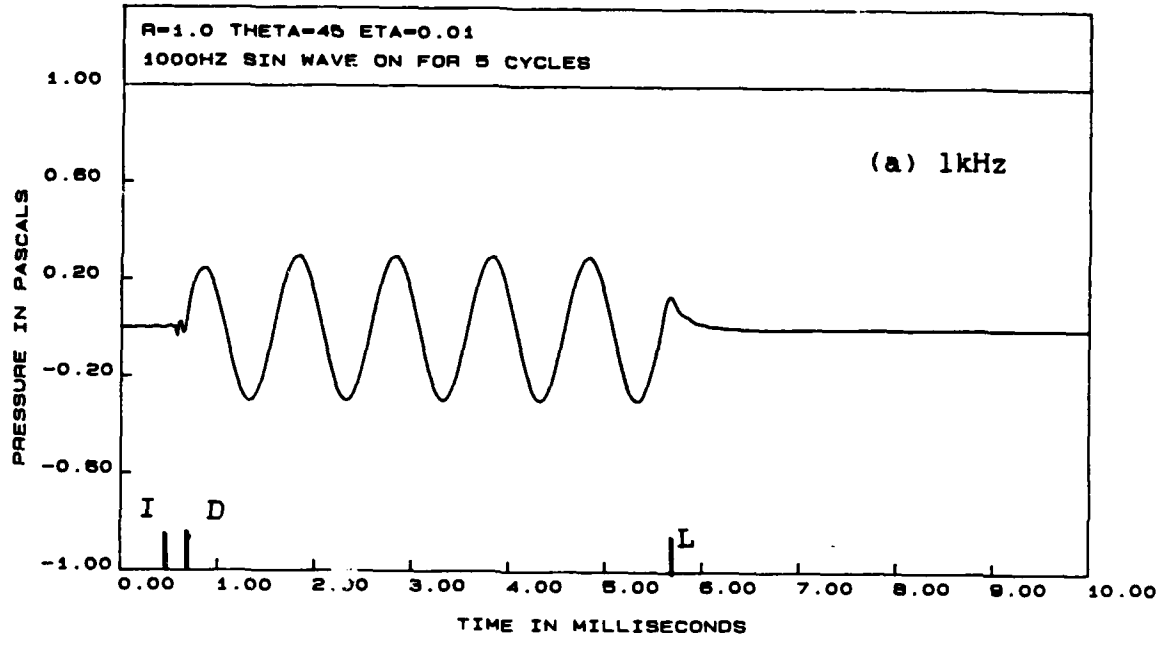

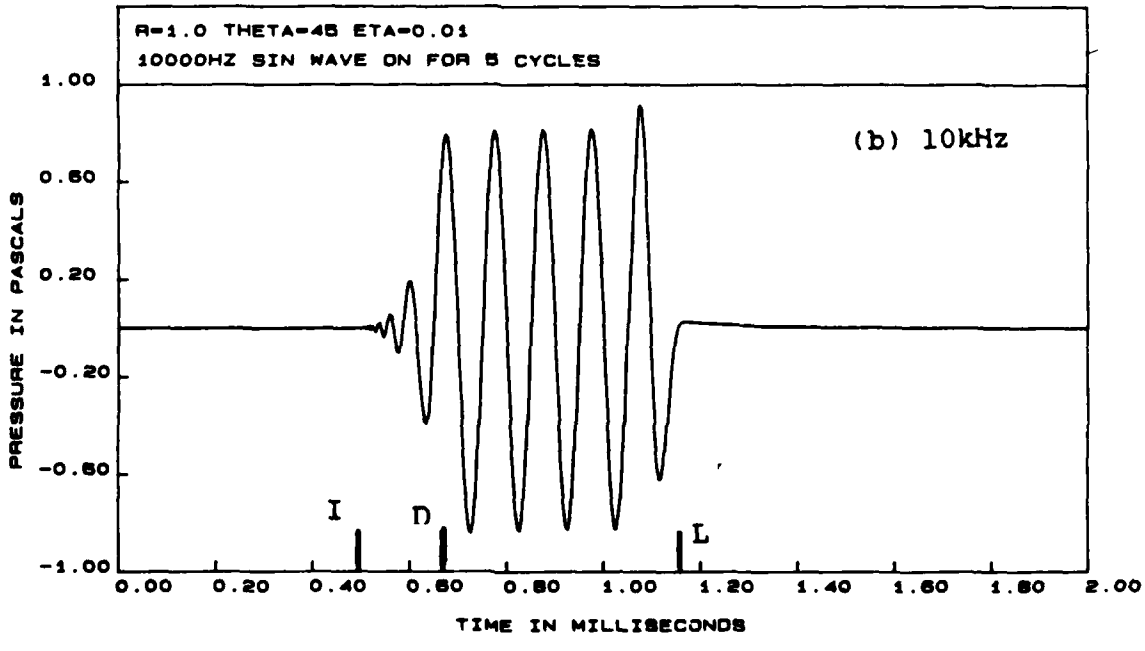

FIG. 3 WARHAM. UNIT SIN WAVE SWITCHED ON FOR 5 CYCLES
R=1.0m θ=45° (a) 1kHz (b) 10kHz

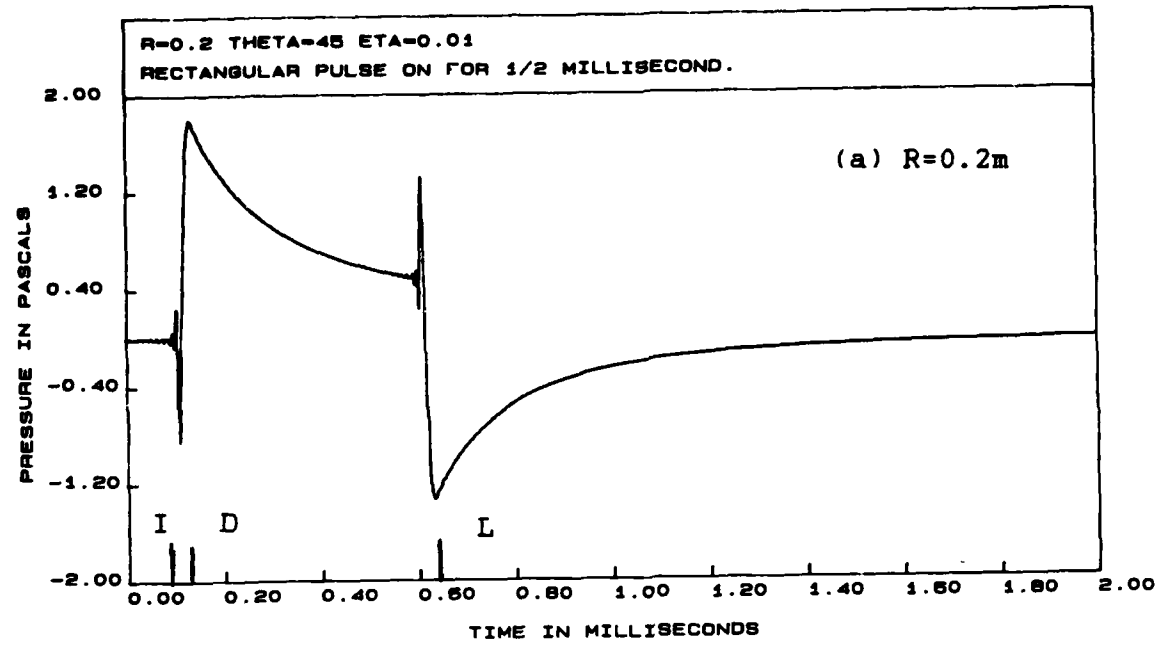

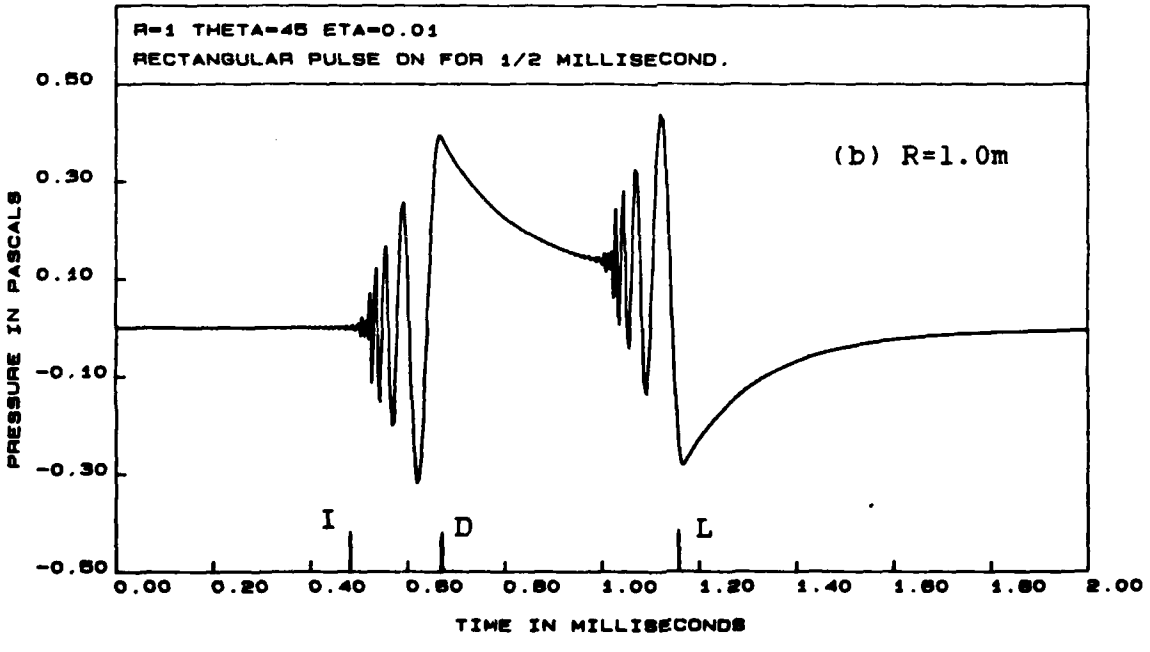

FIG. 4 WARHAM. UNIT RECTANGULAR PULSE EXCITATION
θ=45° (a) R=0.2m (b) R=1.0m.

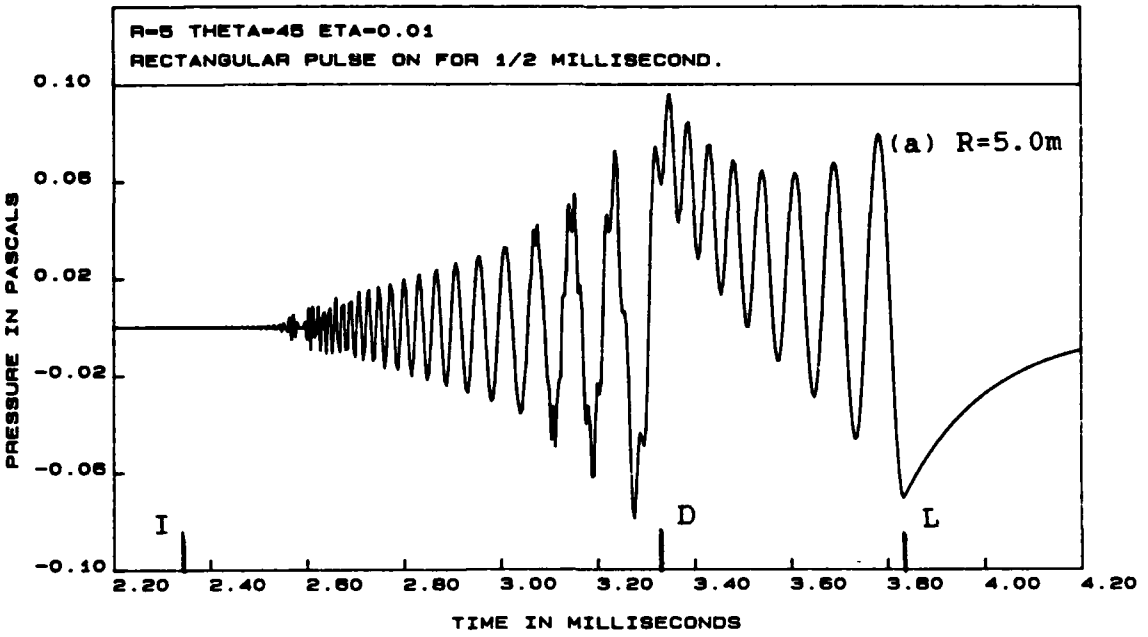

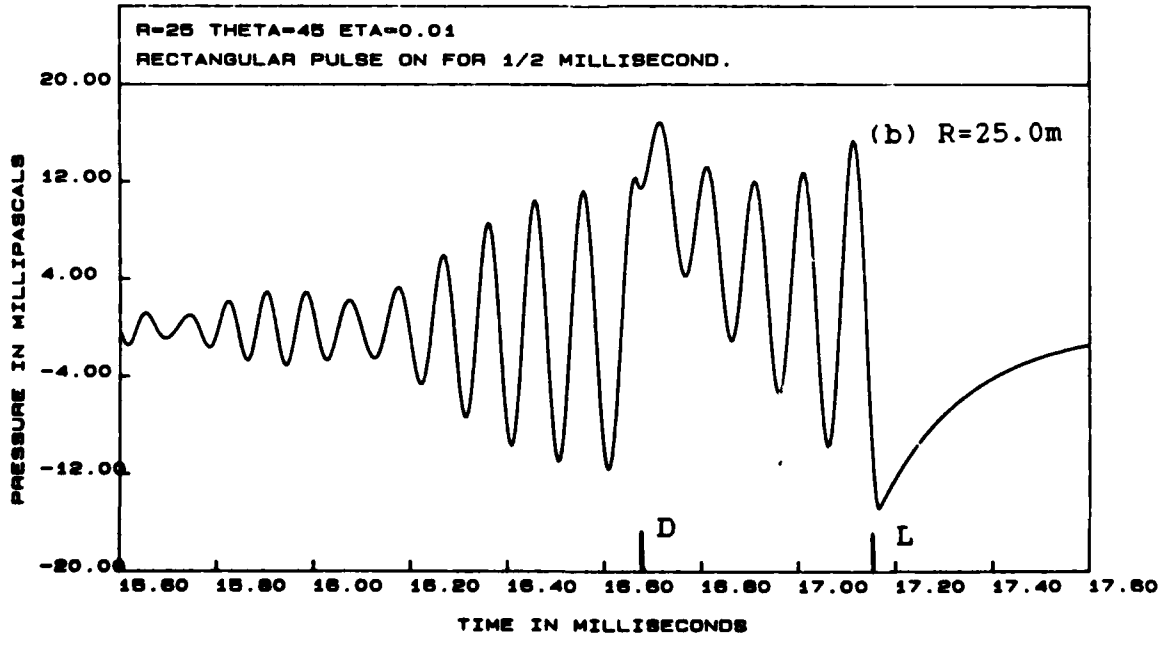

FIG. 5 WARHAM. UNIT RECTANGULAR PULSE EXCITATION
θ=45° (a) R=5.0m (b) R=25.0m

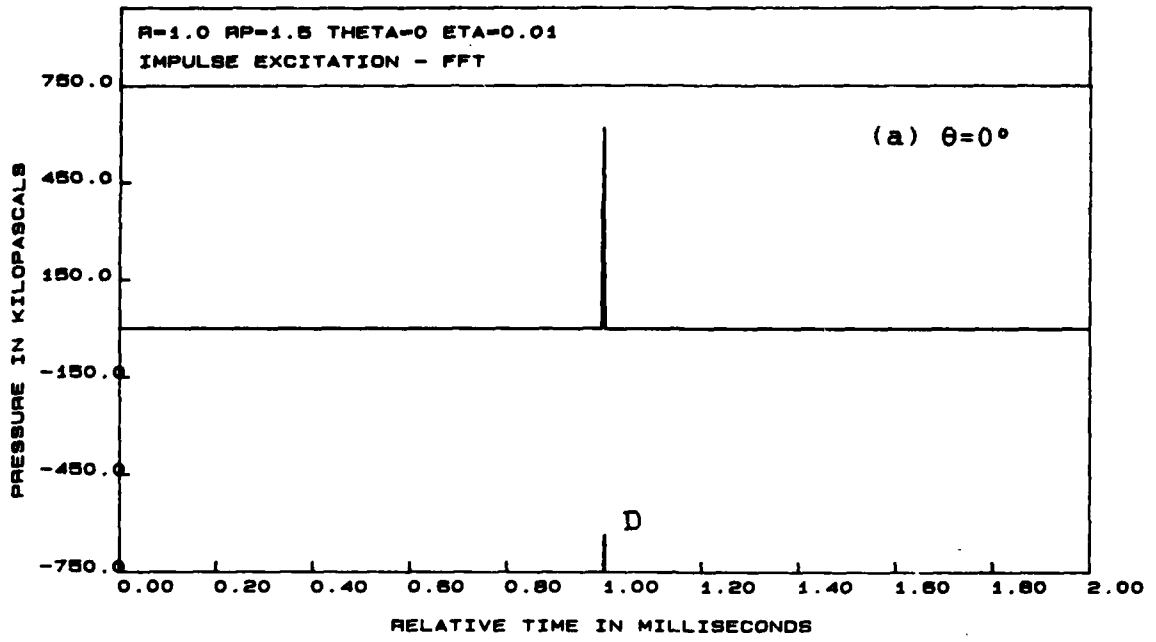

Pressures referred to 1m

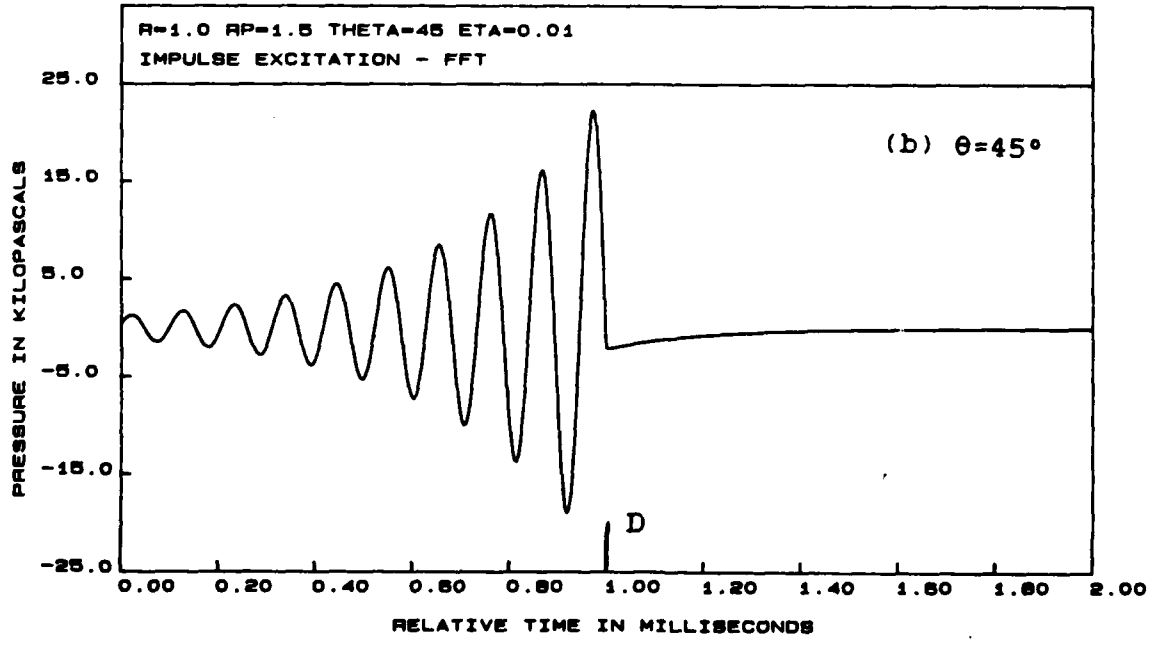

FIG. 6 FFT. EXCITATION IS A UNIT IMPULSE
(a) θ=0° (b) θ=45°

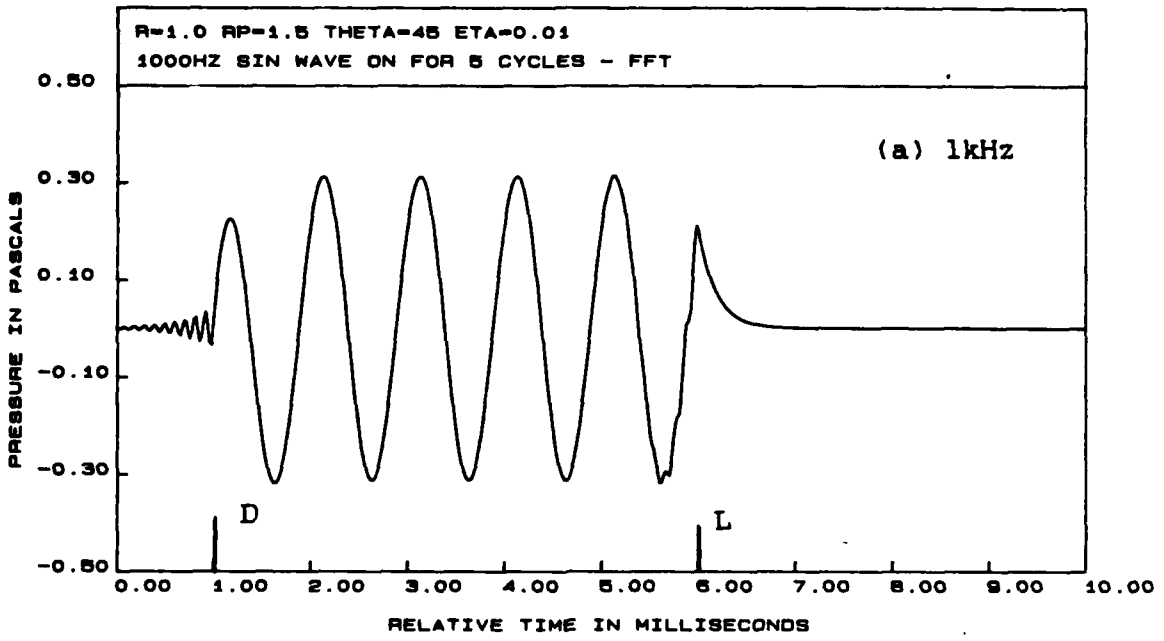

Pressures referred to 1m

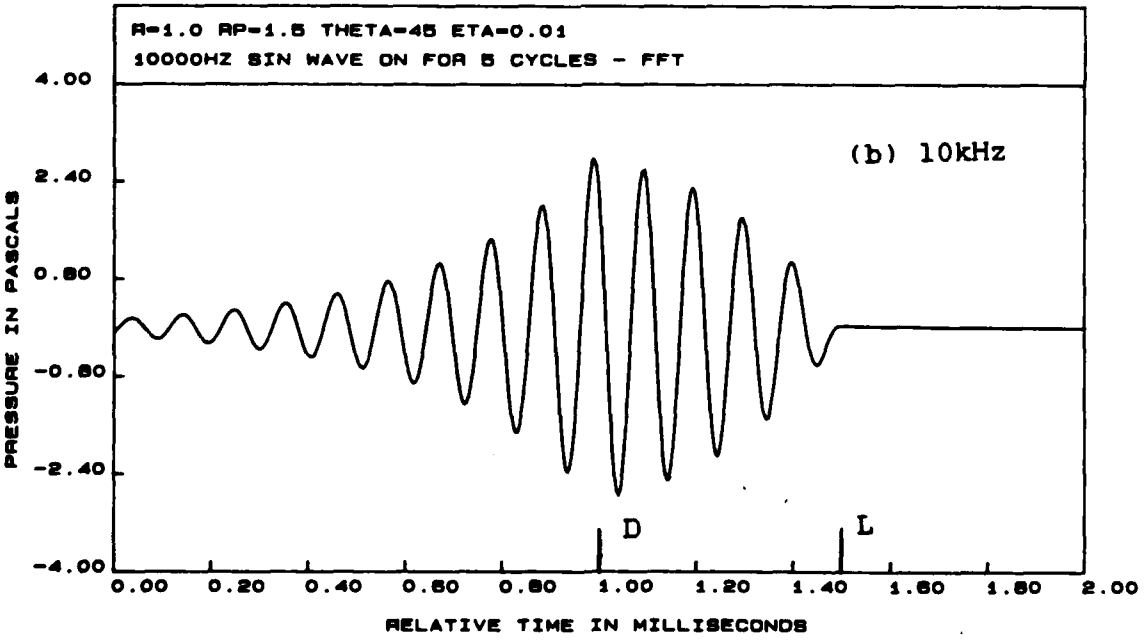

FIG. 7 FFT. UNIT SIN WAVE SWITCHED ON FOR 5 CYCLES
(a) 1kHz (b) 10kHz

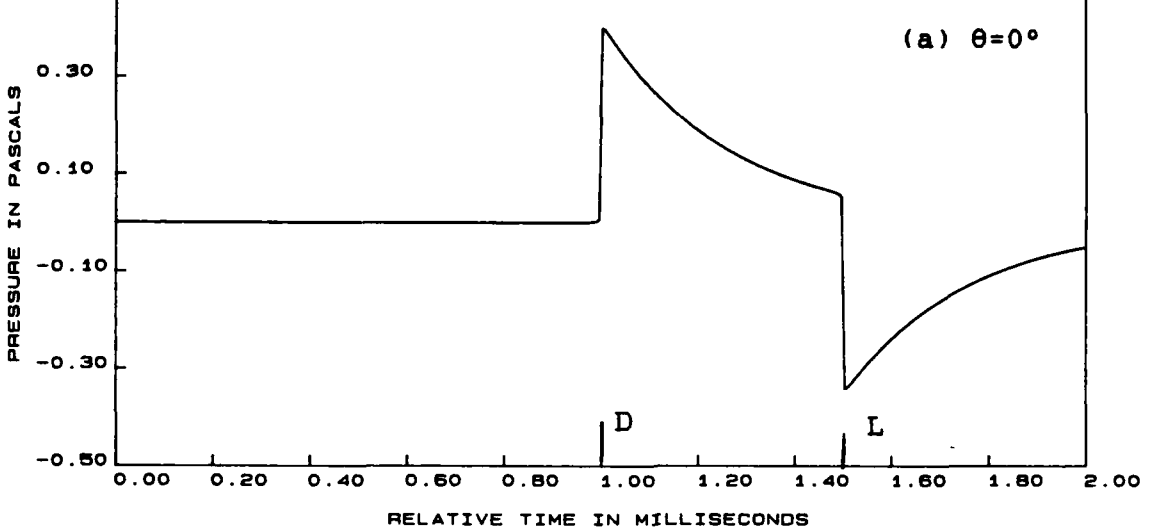

Pressures referred to 1m

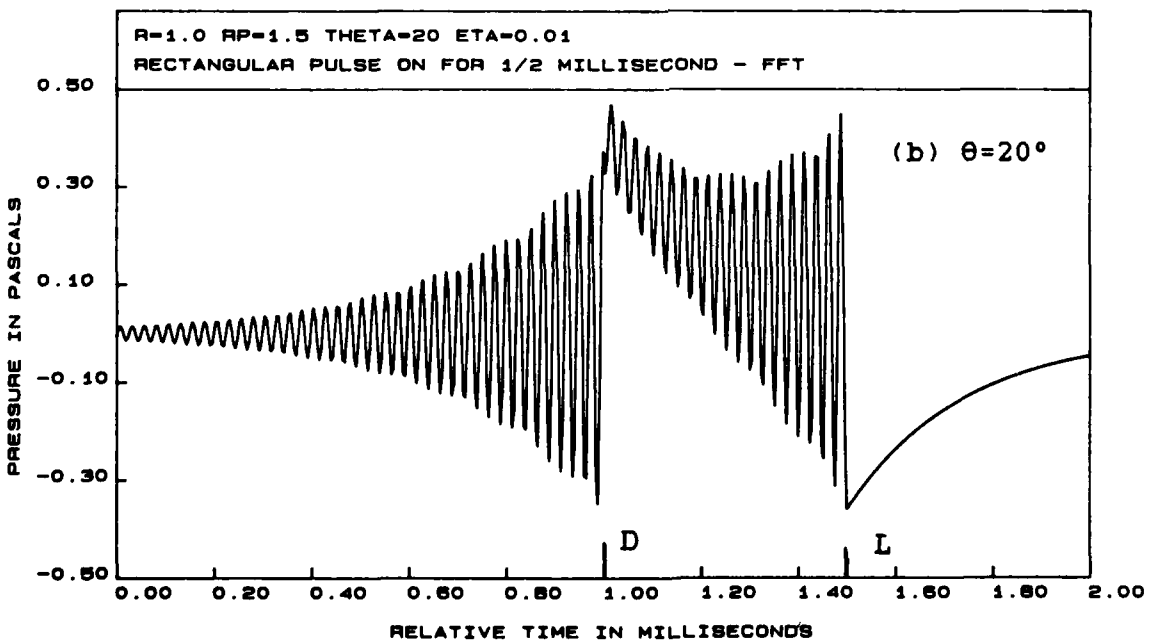

FIG. 8 FFT. UNIT RECTANGULAR PULSE EXCITATION
(a) θ=0° (b) θ=20°

ARE TM(UHA)87508

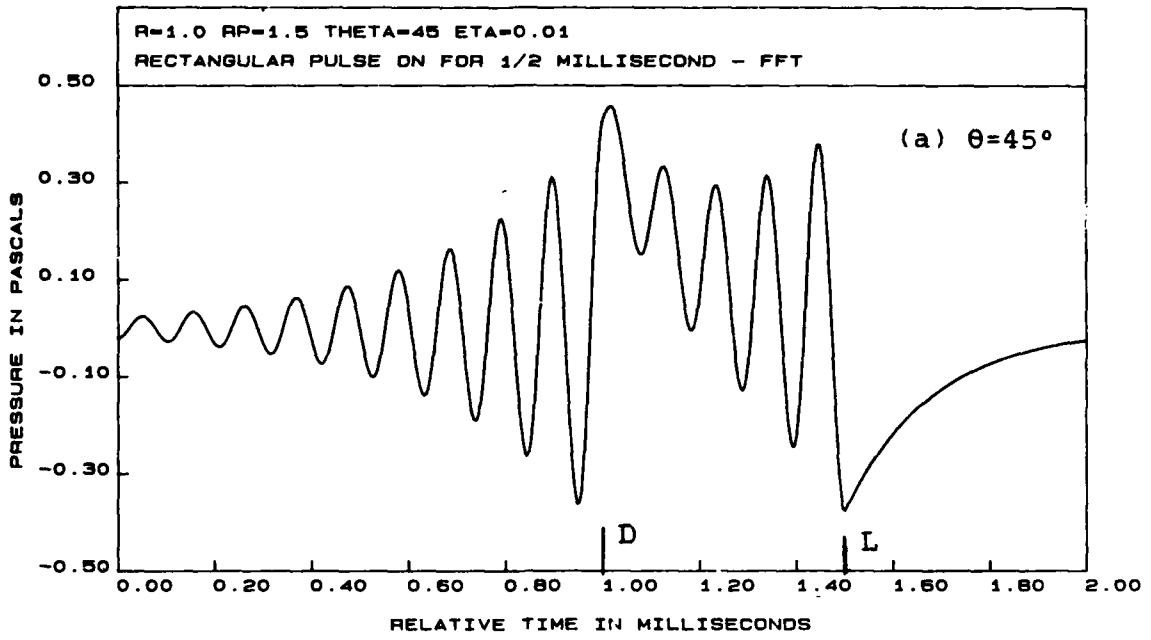

Pressures referred to 1m

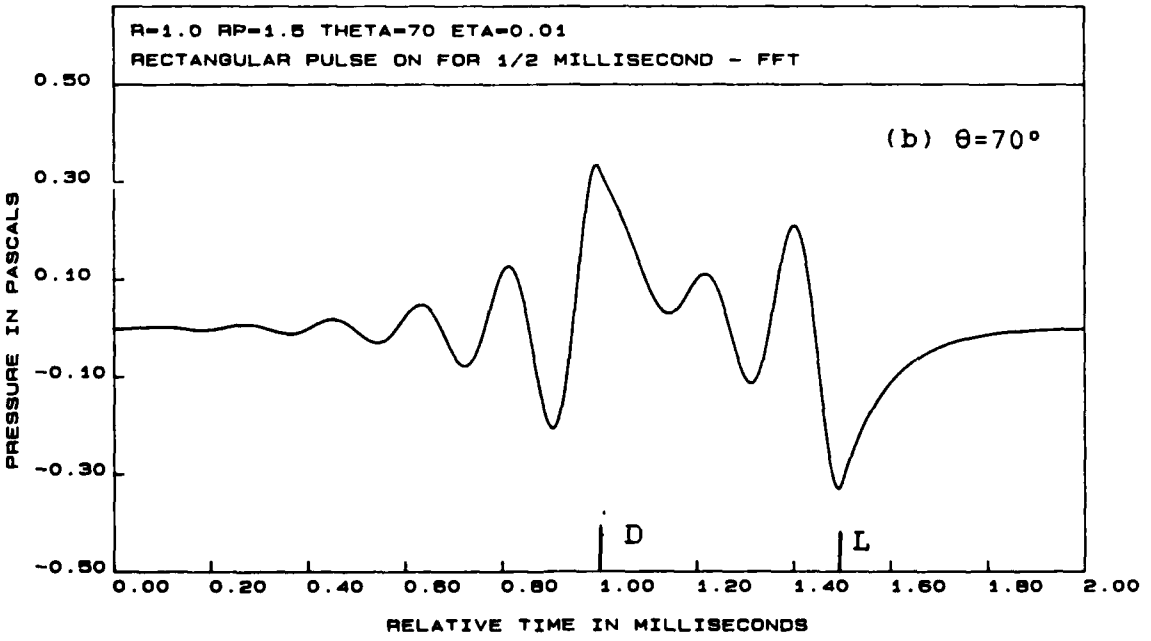

FIG. 9 FFT. UNIT RECTANGULAR PULSE EXCITATION
(a) θ=45° (b) θ=70°

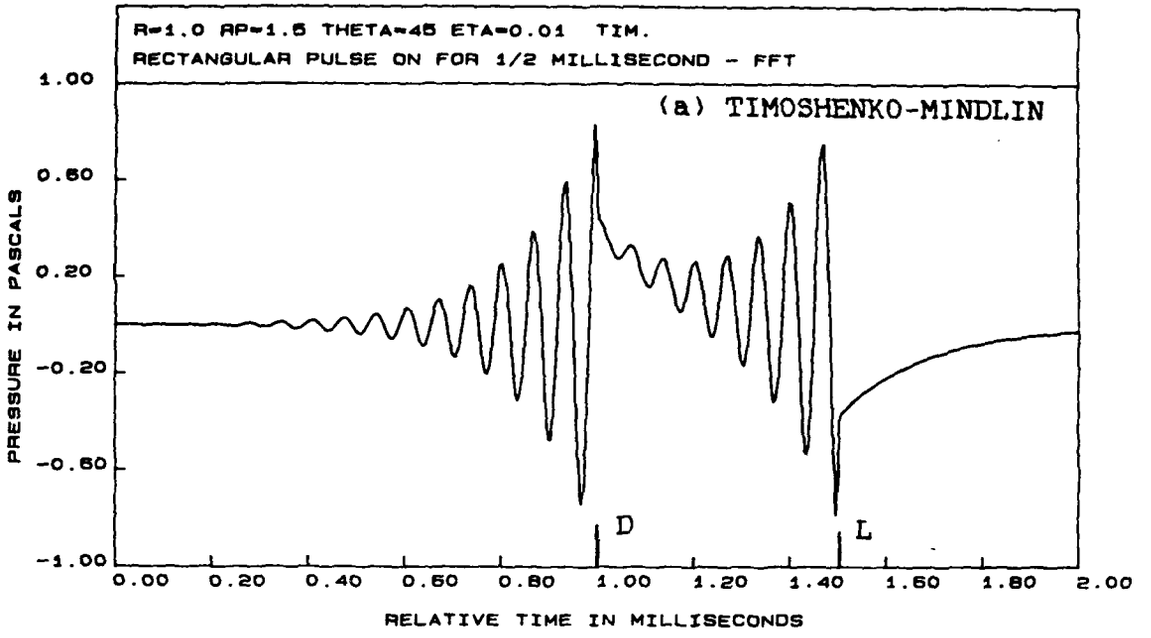

Pressures referred to 1m

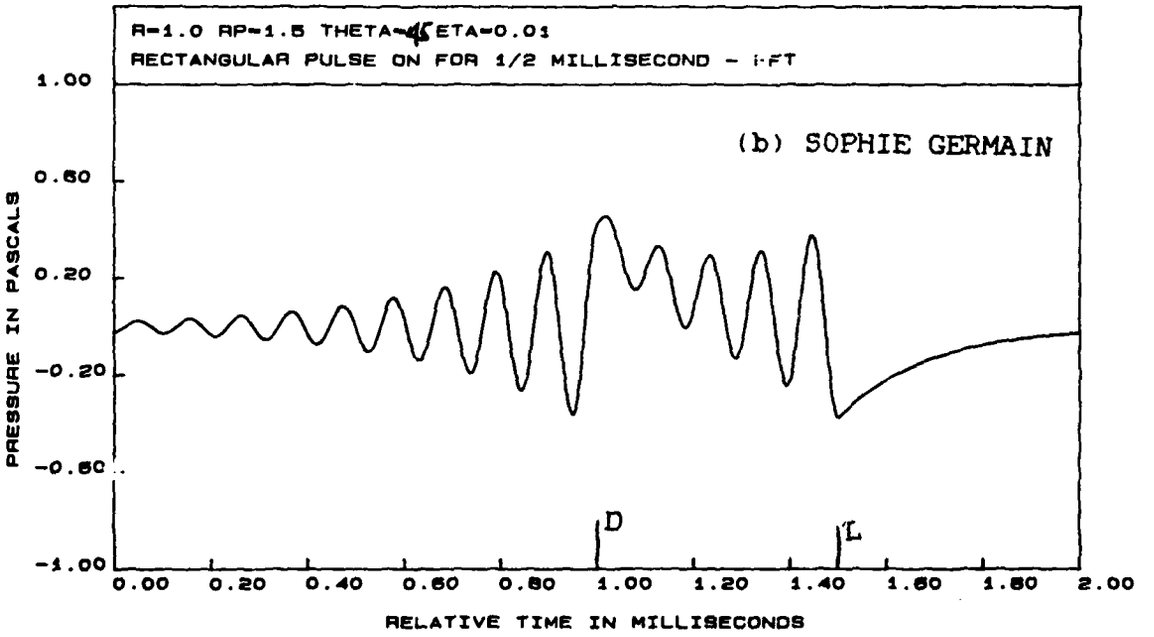

FIG. 10 FFT. COMPARISON OF PLATE THEORIES
UNIT RECTANGULAR PULSE EXCITATION
θ=45° (a) THICK (b) THIN

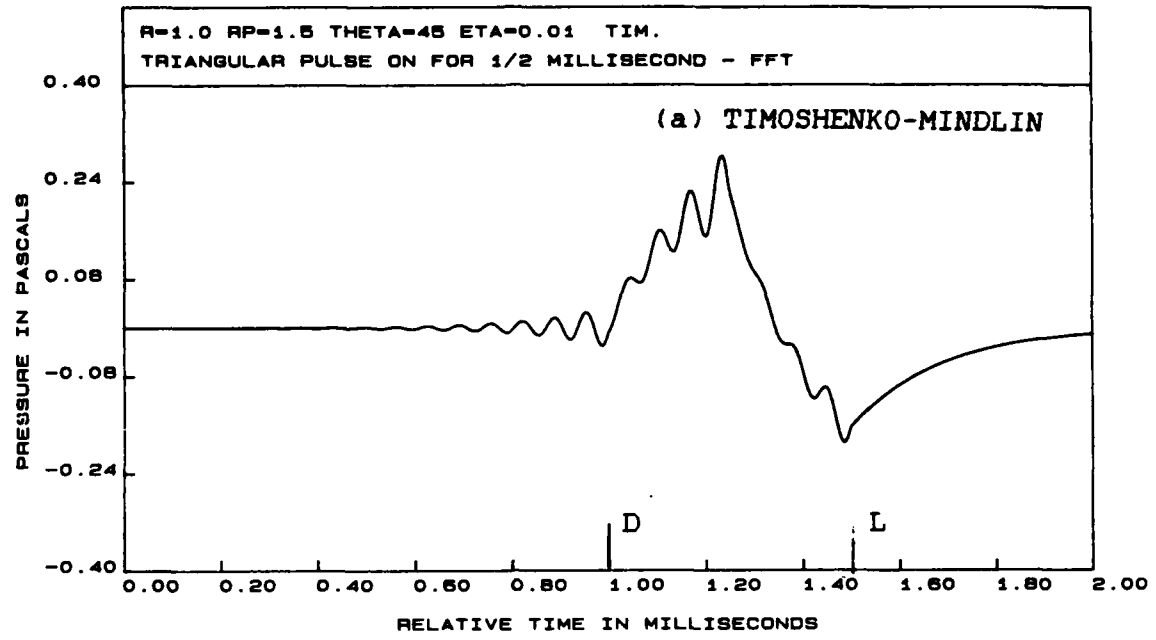

Pressures referred to 1m

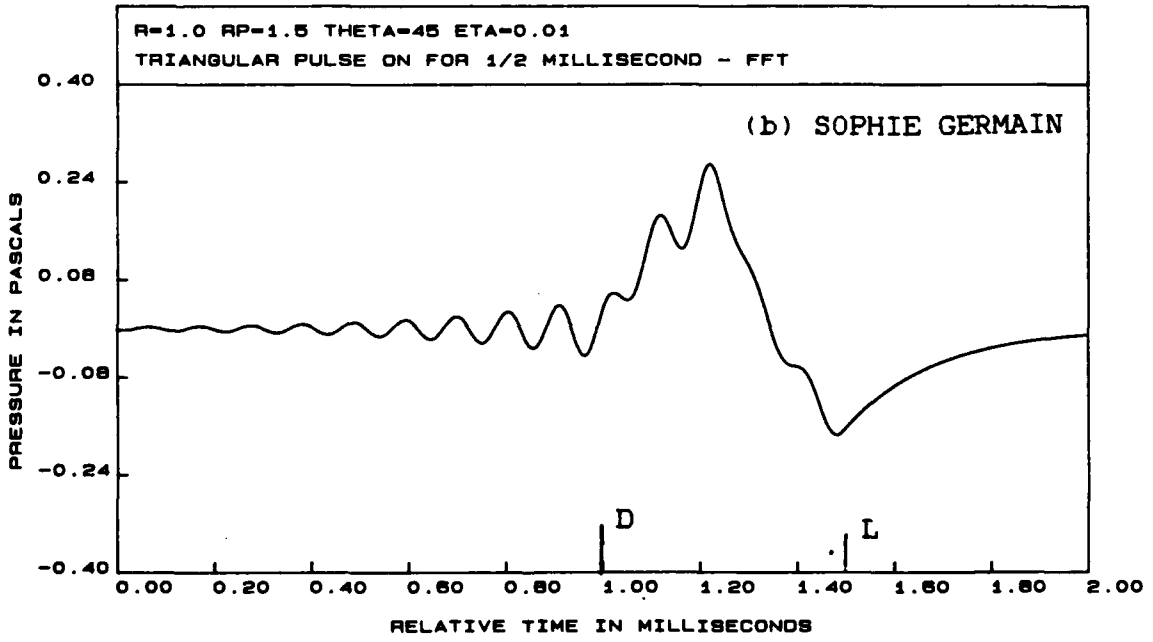

FIG. 11 FFT. COMPARISON OF PLATE THEORIES
UNIT TRIANGULAR PULSE EXCITATION
θ=45° (a) THICK (b) THIN

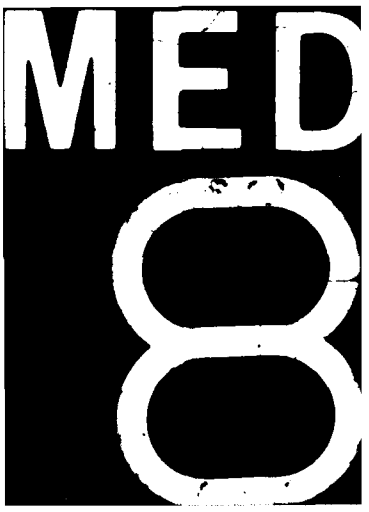
MED
8